

# Effect of Solution Concentration on Optical and Morphological Properties of Gallium Nitride Thin Films

E.S. ALI<sup>a,b,\*</sup>, WISAM J. AZIZ<sup>a</sup> AND ASMIT R. AL-HADDITHI<sup>c</sup>

<sup>a</sup>*Department of Physics, College of Science, Mustansiriyah University, Palestine St., 10052, Baghdad, Iraq*

<sup>b</sup>*Directorate General of Education in Diyala, Ministry of Education, Iraq*

<sup>c</sup>*Department of Physics, College of Science, AL Anbar University, AL Anbar, Iraq*

Doi: [10.12693/APhysPolA.140.354](https://doi.org/10.12693/APhysPolA.140.354)

\*e-mail: [esamsalim@uomustansiriyah.edu.iq](mailto:esamsalim@uomustansiriyah.edu.iq)

The effects of precursor concentration on the structural, morphological, and optical properties of gallium nitride thin films were studied. The films were prepared by depositing solutions with two different precursor concentrations on quartz, *p*-type Si (100), and porous silicon substrates using the chemical spray pyrolysis technique. Gallium nitrate hydrate ( $\text{Ga}(\text{NO}_3)_3 \cdot x \text{H}_2\text{O}$ ) powder dissolved in ethanol was used as the gallium source. Morphological, structural, optical, and spectral properties of the deposited films were characterized by atomic force microscopy, X-ray diffraction, Raman spectroscopy, photoluminescence, and ultraviolet–visible spectrophotometry. The X-ray diffraction results showed a hexagonal structure with orientation normal to the (004) plane. The optical bandgap decreased from 3.17 eV to 3.1 eV when the precursor concentration increased. The results from atomic force microscopy demonstrated that the grain sizes increased from 35 nm to 50 nm when the concentration increased. The root-mean-square also increased, from 9.666 nm to 12.4 nm, as the concentration increased. Blue photoluminescence of gallium nitride was detected in the range from 380 nm to 480 nm and Raman results showed a peak centered at  $710 \text{ cm}^{-1}$ , consistent with the GaN longitudinal optical phonon  $A_1$  of wurtzite structure.

topics: chemical spray pyrolysis, gallium nitride

## 1. Introduction

Gallium nitride (GaN) is an important group III–V semiconductor due to its wide, direct bandgap (approximately 3.44 eV at 293 K). It is known to be effective in laser diodes (LD) used for high optical storage [1]. In addition, it has a high electrical breakdown field and excellent thermochemical stability, resulting in successful application in detectors operating in ultraviolet (UV) as well as high frequency and high power devices [2]. GaN increases the efficiency of solar electric operations to above 40% and reduces the cost of large-scale solar electricity generation [3].

Various techniques can be used to synthesize GaN films, including chemical vapour deposition, molecular beam epitaxy, spin coating, dip coating, spray pyrolysis, and vapor phase epitaxy [4, 5]. Chemical spray pyrolysis is a processing method used in research to prepare thin and thick films of ceramic coatings and powders because it is inexpensive and the sprinkler system components are straightforward, easy to use, and safe. It is an effective technique for making films of any composite [6]. The basic thermal chemical deposition system includes

a vaporizer, precursor solution, substrate heater, and thermocouple [12]. The structural properties of the deposited films are determined by the main spray pyrolysis parameters, including the temperature of the substrate, precursor solution, type of raw material used, and its concentration in the precursor solution. Furthermore, the presence of additives, nozzle to substrate distance, solution flow rate, and atomization rate influence the physical and chemical properties of the film [7]. The aim of this study was to determine the effect of precursor concentration on the structural properties of GaN thin films.

## 2. Materials and methods

### 2.1. Precursor preparation and deposition parameters

Two spray solutions with precursor concentrations of 0.06 M and 0.12 M were prepared by the following procedure. Gallium nitrate hydrate powder ( $\text{Ga}(\text{NO}_3)_3 \cdot \text{H}_2\text{O}$ ) was dissolved in 120 ml ethanol ( $\text{C}_2\text{H}_5\text{OH}$ ) by stirring at room temperature for 40 min. Substrates were cleaned in an ultrasonic bath using ethanol and distilled water for 20 min

and dried in hot air. Compressed air (4 bar) was used to atomize the solution onto the substrates (quartz SiO<sub>2</sub> *p*-type silicon Si (100), and porous silicon (PS) at 200°C for 10 s, with a 20-s pause between samples. The thin films were annealed for 2 h under ammonia flow at 900°C in a tube furnace.

### 2.2. Thin film characterization

The film's surface morphology was investigated using atomic force microscopy (AFM). A double beam spectrophotometer UV-260 (from Spectro-BioTech) was used to study transmittance within the 300–1200 nm range. Raman and photoluminescence (PL) spectra were measured with use of a Sunshine (V2-86) spectrometer. X-ray diffraction (XRD) was used to determine the crystallographic structure of the samples.

## 3. Results and discussion

### 3.1. X-ray diffraction results

Figure 1 shows the XRD spectra of the GaN nanostructures grown on silicon at 200°C. The indexed diffraction peaks in Fig. 1 are consistent with the JCPDS data for hexagonal GaN. The peaks representing the crystalline planes (102), (110), (103), (200), (112), and (004) are located at 47.61°, 56.44°, 61.8°, 66.347°, 72.13°, and 75.02°, respectively. From the position of the (004) peak the lattice constant  $c = 32.802$  Å was determined.

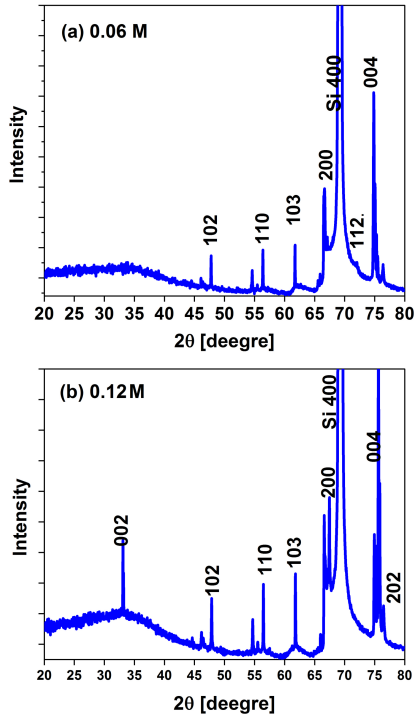


Fig. 1. X-Ray diffraction patterns of the GaN films for (a)  $C = 0.06$  M and (b)  $C = 0.12$  M.

TABLE I

Root mean square of GaN prepared for concentration values of  $C = 0.06$  M and  $C = 0.12$  M on to different substrates.

Sample	$C$ [M]	Skewness $S_{sk}$	Root mean square [nm]	Kurtosis $S_{ku}$
GaN/quartz	0.06	0.7255	9.566	2.641
GaN/quartz	0.12	-0.7568	12.44	4.302
GaN/Si	0.06	-0.9449	9.592	3.675
GaN/Si	0.12	0.1230	12.46	2.561
GaN/Ps	0.06	-0.198	9.371	2.342
GaN/Ps	0.12	-0.5582	14.27	3.012

The average crystallite size was found to be 21.853 nm. The intense peak at 69.24° corresponds to the (400) reflex of the Si substrate. Some peaks not consistent with GaN, located at  $2\theta$  equal to 46.39°, 57.4°, and 65.93°, correspond to the crystalline phase of gallium oxide Ga<sub>2</sub>O<sub>3</sub>.

### 3.2. Morphological properties

The surface topography of the deposited GaN films was determined using AFM which provides information about the film's structure, grain size, and surface roughness. Figure 2 shows the two- and three-dimensional atomic force microscopy images for a  $20 \times 20$  μm area. The images revealed that application of the 0.12 M solution resulted in a homogenous surface that was much smoother than that obtained with the lower concentration, i.e., 0.06 M. This result indicates that with increasing solution molarity, the uniformity of the coating increases. The grain size increased from 40.44 nm to 58.2 nm, and the root-mean-square increased from 9.592 nm to 12.46 nm.

Table I shows the root-mean-square of AFM analysis. Skewness ( $S_{sk}$ ) that characterizes the spatial distribution of height variation for thin films was generally negative when GaN concentration increased, indicating the presence of deep valleys or pits. Kurtosis ( $S_{ku}$ ), which describes the uniformity of height variations, increased when the concentration of the solution increased, indicating an increase in the number of peaks.

### 3.3. Raman spectrum

Figure 3 shows Raman spectra of GaN thin films deposited on Si and PS substrates, collected using a light source with a wavelength of 532 nm. The Raman spectra were compared to the vibrational density of states computed for hexagonal GaN. The peak at 710 cm<sup>-1</sup> is attributed to the longitudinal optical phonon  $A_1$  (LO) and the peak near 576 cm<sup>-1</sup> is consistent with the  $E_2$  (high) mode of wurtzite GaN. The energy of the  $E_2$  (low) mode is 400 cm<sup>-1</sup> lower than that of the latter and thus

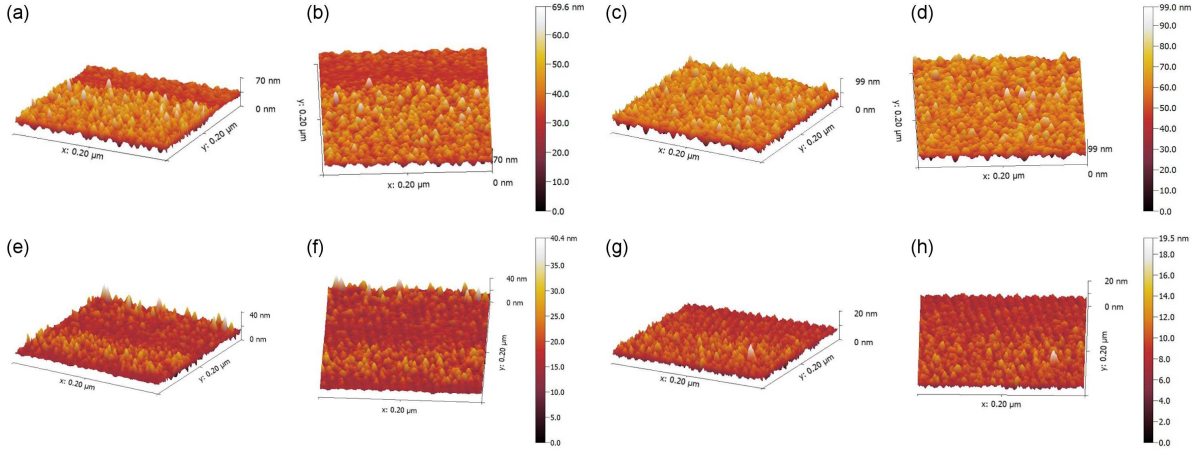


Fig. 2. AFM of GaN films deposited on (a) Si for 0.06 M, 3D, (b) Si for 0.06 M, 2D, (c) Si for 0.12 M, 3D, (d) Si for 0.12 M, 2D, (e) porous Si for 0.06 M, 3D, (f) porous Si for 0.06 M, 2D, (g) porous Si for 0.12 M, 3D, (h) porous Si for 0.12 M, 2D.

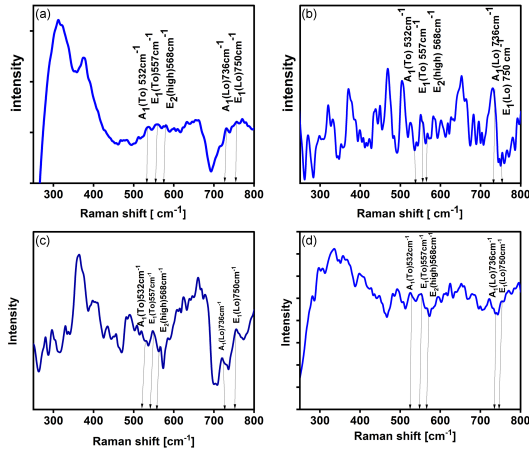


Fig. 3. Raman spectra at room temperature of GaN films deposited on Si (a, b) and porous Si (c, d) substrates with precursor solution concentrations of  $C = 0.06$  M (a, c) and  $C = 0.12$  M (b, d).

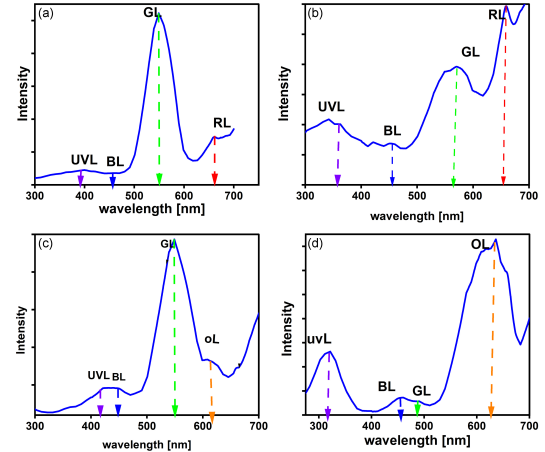


Fig. 4. Room temperature PL spectra of GaN films deposited on (a, b) Si and (c, d) porous Si substrates for precursor concentrations of (a, c)  $C = 0.06$  M and (b, d)  $C = 0.12$  M, respectively.

not detected in the experiment. The broad band at low frequencies is due to combination of acoustic and optical phonons. The film showed structure in both bands consistent with the main GaN modes.

### 3.4. Photoluminescence spectra

Figure 4 shows the photoluminescence (PL) of GaN films formed on different substrates in the 200–900 nm wavelength range. The wavelength of light employed for excitation was 190 nm. The emission at wavelengths below 360 nm stems from the crystalline phase of  $\text{Ga}_2\text{O}_3$ , detected in X-ray diffraction. The broad violet-blue (BL), green (GL), and red (RL) luminescence bands are due to the near bandgap emission of GaN, and the existence of Ga and N vacancies, oxygen or deep level impurities, and amorphous phases [8]. When the GaN precursor concentration increased from 0.06 to 0.12 M, the PL peak positions and intensities

changed. In particular, the near bandgap emission of GaN shifted slightly towards higher wavelengths. Nevertheless, it agrees well with the emission spectra of GaN layers deposited with other techniques [10–12]. In addition, we observed a yellow luminescence band near 500–600 nm caused by defects or impurities.

### 3.5. UV–VIS spectroscopy

Figure 5a shows the transmittance spectra for the two precursor concentrations of GaN thin film deposition. The transmittance decreased as the precursor concentration increased. The films were transparent in the wavelength range from 350 nm to 700 nm. In addition, the transmittance was 90% for the lower precursor concentration, while for the higher concentration it was approximately equal to 75% [13, 14]. Figure 5b shows that the optical

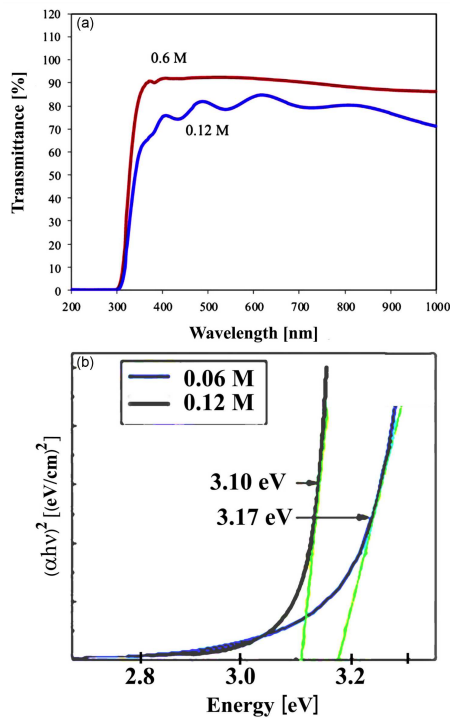


Fig. 5. (a) Transmittance of GaN films for precursor concentrations of 0.12 M and 0.06 M. (b) Square of the product of the absorption coefficient and photon energy vs photon energy for the same films.

band gap of GaN decreased when precursor concentrations increased, i.e., from 3.17 eV at 0.12 M to 3.1 eV at 0.06 M. These values are a little lower than in crystalline layers but are consistent with other reports [15, 16].

#### 4. Conclusions

GaN thin films were deposited from solutions with two different precursor concentrations, using a simple and low-cost spray pyrolysis technique. The X-ray diffraction results showed that the films were polycrystalline. The crystallites had a wurtzite structure and orientation (004). AFM images revealed the nature of the surface of the GaN thin films, i.e., surface waviness, a valley region of relatively medium roughness, and in certain orientations, a hill region. Kurtosis  $S_{ku}$  increased with increasing concentration and negative values of skewness  $S_{sk}$  were present, indicating the existence of pits and depressions when concentration increased. The root-mean-square increased. The optical transmittance decreased with increased concentration. In optical examinations, a direct bandgap appeared, the value of which changed proportionally with the concentration of the precursor solution from 3.17 to 3.1 eV. Raman spectra analysis showed that the peak near  $710\text{ cm}^{-1}$  was consistent with the vibration frequency of the GaN phonon. Finally, the PL measurement was in agreement with the known wavelength region of GaN.

#### Acknowledgments

The authors would like to thank Mustansiriyah University (see [www.uomustansiriyah.edu.iq](http://www.uomustansiriyah.edu.iq)) Baghdad Iraq for its support in the present work.

#### References

- [1] P. Moses, M. Miao, Q. Yan, C. Van de Walle, *J. Chem. Phys.* **134**, 084703 (2011).
- [2] H. Maizatul, S. Ng, *J. Phys. Conf. Series* **1535**, 012038 (2020).
- [3] A. McInnes, J. Sagu, K. Wijayantha, *Mater. Lett.* **137**, 214 (2014).
- [4] K. Yu, M. Ting, S. Novikov, C. Collin, W. Sarney, S. Svensson, *J. Phys. D* **48**, 385101 (2015).
- [5] E. Gastellóu, G. García, A. Herrera, C. Morales, R. García, G. Hirata, *ApplSci.* **11**, 6990 (2021).
- [6] E. Gastellóu, C. Morales, G. García, R. García, G. Hirata, A. Herrera, *J. Alloys Compd.* **783**, 927 (2019).
- [7] E. Gastellóu, C. Morales, G. García, R. García, G. Hirata, A. Herrera, *Opt Mater.* **88**, 277 (2019).
- [8] E. Gastellóu, C. Morales, R. García, G. García, G. Hirata, A. Herrera, *J. Alloys Compd.* **772**, 1024 (2019).
- [9] H. Xiao, R. Liu, J. Liu, Z. Lin, L. Mei, *Vacuum* **83**, 1393 (2009).
- [10] T. Honda, Y. Inao, K. Konno, K. Mineo, S. Kumabe, H. Kawanishi, *Phys Status Solidi A* **192**, 461 (2002).
- [11] V. Rangel-Kuoppa, C. Aguilar, V. Sánchez-Reséndiz, *Thin Solid Films* **519**, 2255 (2011).
- [12] L. Martínez-Ara, J., Aguilar-Hernández, J. Sastré-Hernández, L. Hernández-Hernández, M. Hernández-Pérez, P. Maldonado-Altamirano, *Mater. Res.* **22**, e20180263 (2019).
- [13] X. Zeng, B. Han, X. Wang, J. Shi, Y. Xu, J. Zhang, J. Wang, K. Xu, *J. Cryst. Growth Des.* **367**, 48 (2013).
- [14] A. McInnes, J. Sagu, D. Mehta, K. Wijayantha, *J. Sci Rep.* **9**, 2313 (2019).
- [15] S. Kazazis, E. Papadomanolaki, M. Androulidaki, K. Tsagaraki, A. Kostopoulos, E. Aperathitis, E. Iliopoulos, *Thin Solid Films* **611**, 46 (2016).
- [16] P. Brack, J. Sagu, T. Peiris, A. McInnes, M. Senili, K. Wijayantha, *J. Chem. Vap. Depos.* **21**, 41 (2015).